

<https://helda.helsinki.fi>

Addressing criticalities in the INFOGEST static in vitro digestion protocol for oleogel analysis

Sabet, Saman

2022-10

Sabet , S , Kirjoranta , S , Lampi , A-M , Lehtonen , M , Pulkkinen , E E & Valoppi , F 2022 , ' Addressing criticalities in the INFOGEST static in vitro digestion protocol for oleogel analysis ' , Food Research International , vol. 160 , 111633 . <https://doi.org/10.1016/j.foodres.2022.111633>

<http://hdl.handle.net/10138/347004>

<https://doi.org/10.1016/j.foodres.2022.111633>

cc_by

publishedVersion

Downloaded from Helda, University of Helsinki institutional repository.

This is an electronic reprint of the original article.

This reprint may differ from the original in pagination and typographic detail.

Please cite the original version.



Addressing criticalities in the INFOGEST static *in vitro* digestion protocol for oleogel analysis

Saman Sabet^{a,b,*}, Satu J. Kirjoranta^a, Anna-Maija Lampi^a, Mari Lehtonen^a, Elli Pulkkinen^a, Fabio Valoppi^{a,b,c,*}

^a Department of Food and Nutrition, University of Helsinki, P.O. Box 66, FI-00014 Helsinki, Finland

^b Faculty of Agriculture and Forestry, Helsinki Institute of Sustainability Science, University of Helsinki, 00014 Helsinki, Finland

^c Electronics Research Laboratory, Department of Physics, University of Helsinki, Gustaf Hällströmin katu 2, PO Box 64, 00014 Helsinki, Finland

ARTICLE INFO

Keywords:

Oleogel
INFOGEST static *in vitro* digestion
Lipid digestion
Oleogel's digestibility
Gastrointestinal fate of oleogels
INFOGEST protocol for oleogels

ABSTRACT

The interest on the digestive fate of oleogels, i.e., substitutes for solid fats rich in liquid oil, have pushed researchers to use the widely adopted INFOGEST protocol for static *in vitro* digestion. However, this protocol was originally designed to simulate the digestibility of conventional foods and to accommodate the large fraction of oil in oleogels, researchers have deliberately modified the INFOGEST protocol, inadvertently leading to results difficult to be compared.

In this study, we highlighted possible problems that may arise during oleogel simulated digestion such as under- or overestimation of oleogel lipolysis. The effect of oleogel amount, oleogelator type and concentration, and shear applied during digestion on the rate and extent of oleogel digestion was studied. The release of fatty acids during the application of INFOGEST protocol was monitored using the pH-stat method and compared to those analyzed by HPLC-ELSD. Oleogels' structural information was obtained using brightfield, polarized, and fluorescence microscopy, and DSC. We determined that lipolysis of ethylcellulose oleogels follow the "interaction with enzymes and bile salts" pattern, whereas that of wax oleogels follow the "disintegration of oleogel and interaction with enzymes and bile salts". We also observed that the chemical composition of wax, crystal morphology, and crystal distribution do not alter the lipolysis of oil entrapped inside the wax crystals. We finally recommended a few minimal but fundamental modifications to the INFOGEST protocol to achieve more reliable results from the static *in vitro* digestion of oleogels and possibly other lipid-based systems.

1. Introduction

Static, dynamic, and semi-dynamic *in vitro* digestion methods are used to determine the digestion mechanisms of food products by simulating the physiological conditions of the human upper gastrointestinal tract, i.e., oral, gastric, and small intestinal phases. Among them, the static one is the simplest and the least expensive method, which made it the most popular *in vitro* digestion simulation method. However, with an increasing number of researchers adopting *in vitro* digestion, different parameters, such as pH, enzyme and bile salts concentration and activity, composition of simulated digestive fluids and digestion time in their static gastrointestinal methods, were not harmonized (Hur, Lim, Decker, & McClements, 2011), which made results of these studies difficult to compare (Brodkorb et al., 2019). Therefore, the experimental parameters were justified and discussed in detail in relation to available

in vivo physiological data (Dupont et al., 2011), and the harmonized *in vitro* simulated gastrointestinal digestion method was published as the INFOGEST method (Minekus et al., 2014). Five years later this method was amended, improved, and published as the new version of INFOGEST (Brodkorb et al., 2019).

This protocol has been shown to be successful both to increase inter-laboratory reproducibility of results, and to achieve close results to the *in vivo* equivalent, particularly regarding protein digestion and peptide pattern (Egger et al., 2016; Sanchón et al., 2018). Consequently, the INFOGEST method has been extensively applied in order to evaluate the rate and extent of protein, starch, and lipid digestion in conventional foods (e.g., milk powders, bread, meat, and nuts) and model lipoprotein foods (Mat, Le Feunteun, Michon, & Souchon, 2016; Sousa, Portmann, Dubois, Recio, & Egger, 2020; Torcello-Gómez et al., 2020; Zhou, Hu, Tan, Zhang, & McClements, 2021; Egger et al., 2019), to

* Corresponding authors at: Department of Food and Nutrition, University of Helsinki, P.O. Box 66, FI-00014 Helsinki, Finland.

E-mail addresses: saman.sabet@helsinki.fi (S. Sabet), fabio.valoppi@helsinki.fi (F. Valoppi).

<https://doi.org/10.1016/j.foodres.2022.111633>

Received 10 March 2022; Received in revised form 28 June 2022; Accepted 5 July 2022

Available online 8 July 2022

0963-9969/© 2022 The Authors. Published by Elsevier Ltd. This is an open access article under the CC BY license (<http://creativecommons.org/licenses/by/4.0/>).

measure the bioaccessibility of bioactive compounds encapsulated in colloidal delivery systems (Sabet, Rashidinejad, Qazi, & McGillivray, 2021; Tan, Zhang, Mundo, & McClements, 2020; Zhou, Dai, Liu, Tan, Bai, Rojas, & McClements, 2021), to investigate different approaches to reduce lipid digestion, delaying gastric digestion, and providing satiety (Araiza-Calahorra, Glover, Akhtar, & Sarkar, 2020; Infantes-Garcia, Verkempinck, Gonzalez-Fuentes, Hendrickx, & Grauwet, 2021; Verkempinck et al., 2018).

Recently, the INFOGEST protocol has also been used to study the digestion fate of singular food ingredient, such as proteins from plant origin (Santos-Hernández et al., 2020; Sousa et al., 2020; Zhou et al., 2021), polysaccharides (Gallego-Lobillo, Ferreira-Lazarte, Hernández-Hernández, & Villamiel, 2021), and novel lipid-based systems such as oleogels (Ashkar, Laufer, Rosen-Kligvasser, Lesmes, & Davidovich-Pinhas, 2019; Calligaris, Alongi, Lucci, & Anese, 2020; O'Sullivan, 2016b; Wang, Chen, & Liu, 2021). The latter are semi solid gels produced by trapping large fractions of liquid oil (>85%) in a stable three-dimensional network of structuring molecules (Marangoni, van Duynhoven, Acevedo, Nicholson, & Patel, 2020), which attracted the

attention of the scientific and industrial community due to their promising ability to substitute solid fats in food products (Davidovich-Pinhas, Barbut, & Marangoni, 2016) and to deliver lipid-soluble molecules (O'Sullivan, Barbut, & Marangoni, 2016a). However, the INFOGEST protocol was not originally developed for studying the digestion of oleogels which have a high lipid content (>85%), in contrast to conventional foods or delivery systems which contain a limited percentage of lipids (commonly less than 10%). Therefore, to accommodate the large fraction of oil in oleogels, researchers have deliberately modified the INFOGEST protocol. For example, various amount of oleogel and different concentration of lipase and bile salt have been used in gastrointestinal simulation of oleogels (Table 1), compared to the ones mentioned in the original INFOGEST protocol, inadvertently leading to results difficult to be compared. In addition, oleogels are mainly lipophilic elastic gels, which adds additional challenges during the application of the original INFOGEST protocol. For example, oleogels aggregate in the reaction vessel, compared to homogenous conventional foods or emulsions which are commonly used in INFOGEST method. Therefore, oleogels are difficult to disperse and homogenize with the

Table 1

Parameters used during *in vitro* digestion of oleogels found in the literature (INFOGEST method with some modifications and similar methods). The dash (-) means the corresponding data is not mentioned in the article. Based on the *sn*-1,3 specificity of pancreatic lipase (Carey et al., 1983), the 100% free fatty acid release in all of references in this table, is considered as 2/3 of the total FFAs present in the triglycerides.

Type of oleogelator	Oleogelator concentration (wt %)	Type of oil	Amount of oleogel used for digestion simulation (g)	The stirrer bar size/speed in the reaction vessel (rpm)	The small- intestinal lipase activity (U/mL)/ Bile salt concentration in final mixture	Free fatty acid % release from the reference lipid at a certain time	Final free fatty acid % release from the oleogel in similar time as for the oil	Lag time (min)	Reference
Mono- and di-glycerides	8	Canola oil	0.30	-/230	2000/ 187.5 mg	~ 80% in 120 min	77.5 ± 2.1	0	Ashkar et al., 2019 *
	10						82.3 ± 3.3		
	15						91.3 ± 5.9		
	β-sitosterol + γ-oryzanol						28.2 ± 1.2		
	10						39.3 ± 4.7		
	10						34.7 ± 3.8		
Ethyl cellulose 20 cp	15	30.8 ± 0.7							
	8	32.4 ± 2.9							
	10	28.7 ± 1.2							
Ethyl cellulose 45 cp	15	28.4 ± 1.6							
	5	Sunflower oil	0.25	-/-	100/ 80 μmol	~ 54% in 30 min	45.1 ± 0.7	0	Calligaris, Alongi, Lucci, & Anese, 2020
	5						43.1 ± 1.4		
5	32.8 ± 0.7								
Ethyl cellulose 10 cp	10	Canola oil	0.50	-/160	92/ 10 mg/mL	~ 47% in 180 min	39 ± 1	0	O'Sullivan, 2016b **
	10						45 ± 2		
	10						17 ± 2		
Ethyl cellulose 45 cp	10								
	6	Sunflower oil	-	-/-	500/ 10 mM	~ 60% in 120 min	~60	0	Wang, Chen, & Liu, 2021
	8						~70		
10	~80								
Rice bran wax	0.25	Soybean oil	1.6 to 2.0 (gelled oil)	-/-	equivalent 4 × USP specification (-U/mL)/ less than 7.2 mM	~ 90% in 120 min (control is an emulsion containing liquid oil)	~80%	25–40	Guo, Wijarnprecha, Sonwai, & Rousseau, 2019 ***
	0.5						~80%		
	1						~80%		
	4						~90%		

*This study did not follow the INFOGEST protocol. Their model was a modification of Li, & McClements, 2010.

**This study did not follow the INFOGEST protocol. Their model was a modification of Versantvoort, Oomen, Van de Kamp, Rompelberg, & Sips, 2005.

***This study was not on oleogel. It was done on emulsion containing oleogel. This study is shown to demonstrate that the lag time is different compared with other studies where rice bran wax-based oleogels are digested in bulk.

simulated digestive fluids, enzymes, and bile salts. Consequently, the oleogels' lipolysis rate and extent are highly affected by the shear applied to simulate gastrointestinal tract peristalsis. For example, O'Sullivan (2016b) reported the extent of lipolysis (%) for the oleogels made with 10 wt% ethylcellulose (Ethocel 45 cP) at 160 rpm and 200 rpm to be 17 ± 2 and 36 ± 2 , respectively, which further shows the impact of shear on the lipolysis rate and extent of oleogels. However, researchers have used considerably different shear (stirrer bar size and speed, Table 1), which in return caused a decrease in lab-to-lab reproducibility and complicate the comparison of the results. Therefore, there is the need for a harmonized static *in vitro* digestion protocol for oleogels. The sooner a harmonized static *in vitro* digestion protocol is applied by researchers in this field, the more reproducible and comparable the results obtained will be.

In this study, we highlighted possible problems that may arise during oleogel simulated digestion such as under- or overestimation of oleogel lipolysis. The effect of oleogel amount, oleogelator type and concentration, and shear applied during digestion on the rate and extent of oleogel digestion was studied. Then, a few minimal but fundamental modifications are recommended to the INFOGEST protocol to achieve more reliable results from the static *in vitro* digestion of oleogels.

2. Materials and methods

2.1. Materials

Bile bovine (dried, unfractionated B3883), $\text{CaCl}_2(\text{H}_2\text{O})_2$, NaOH, HCl, KCl, KH_2PO_4 , NaCl, $\text{MgCl}_2(\text{H}_2\text{O})_6$, $(\text{NH}_4)_2\text{CO}_3$, sodium taurodeoxycholate, BSA, CaCl_2 , Tris (hydroxymethylaminomethane), tributyrin (purity $\geq 99\%$), and Pancreatin (8 \times USP specifications P7545) from porcine pancreas were obtained from Sigma–Aldrich Co. (Finland). Bile acid kit (1 2212 99 90 313, DiaSys Diagnostic System GmbH, Germany, MAK309-1KT) was purchased from Merk (Finland). Ethyl Cellulose (EC) (45 cP; ETHOCEL™ STD. 45) was purchased from Colorcon Limited (England). Sunflower seed wax (SFW), Rice bran wax (RBW), Candelilla wax (CLW), Carnauba wax (CAW), and Berry wax (BW) were kindly donated by KahlWax (Germany). Sunflower oil was purchased from a local supermarket and kept refrigerated until used. The remaining chemicals used were of analytical quality. Milli-Q® 18.2 MΩ cm water was used to prepare the bolus.

2.2. Oleogel preparation

Viscous oil containing EC 45 cP (5 wt%) and oleogels containing EC45 cP (10, and 15 wt%), or SFW (5 wt%), RBW (5 wt%), CLW (5 wt%), CAW (5 wt%), and BW (5 wt%), or a mixture of EC (5 wt%) and a wax (5 wt%) were prepared by weighing the oleogelator(s) and sunflower oil in a 50 mL beaker. In the case of viscous oil or oleogels with EC and EC plus waxes, the mixture was heated up on a hot plate until they reached 180 ± 5 °C and kept at this temperature for 15 min for complete dissolution of the gelators, while stirring at 100 rpm. Then, the samples were quiescently cooled at room temperature and left to rest overnight. In the case of oleogels made without EC, the mixture was heated to 88 ± 2 °C and kept at this temperature for 5 min under stirring at 100 rpm. Again, the samples were cooled at room temperature overnight. It should be noted that all samples are elastic gels except the 5 wt% EC in oil which is a viscous liquid.

2.3. Polarized and brightfield microscopy

Samples were prepared by depositing a drop of gel onto a glass microscope slide. The gel was gently pressed with a glass cover slip. Imaging was performed using an AxioScope A1 microscope in polarized and brightfield mode (Zeiss Microscopy, Germany) using an AxioCam 305 color camera (Zeiss, Germany). Images were acquired using ZEN 3.2 software (Zeiss, Germany) and a 20X/0.45 Ph2 objective lens (Zeiss,

Germany) at room temperature. All samples were prepared in duplicate and at least 5 images per sample were obtained, and processed using ImageJ software (NIH, USA).

2.4. *In vitro* gastrointestinal tract model

Before applying the gastrointestinal digestion simulation, lipase activity of the pancreatic enzyme was measured based on the previous method (Brodkorb et al., 2019), and resulted to be at 76 U mg^{-1} . Bile salt concentration was also measured with the commercial kit and resulted to be 1.4 mmol g^{-1} . EC oleogel samples were chopped by a knife to pieces of around 2 mm in length, and wax oleogel samples were mixed using a spatula until a mashed potato-like structure was achieved, before they were digested using the INFOGEST standardized static *in vitro* -gastrointestinal digestion simulation (Brodkorb et al., 2019) with some modifications. Oral α -amylase and gastric pepsin have not been utilized in this model, as none of the materials in these experiments were susceptible to these enzymes. In our model, there is a lack of gastric lipase.

2.4.1. First trial: The INFOGEST protocol under low and high shear

In the first trial experiments the amount/fraction of lipid and enzymes were followed as it is mentioned by static *in vitro* INFOGEST protocol (Brodkorb et al., 2019). Briefly, 5 g of sunflower oil or viscous oil (oil containing 5 wt% EC) or oleogel was mixed gently with 5 g of preheated (37 °C) simulated saliva fluid (SSF) in a 50 mL glass beaker. After adding $\text{CaCl}_2(\text{H}_2\text{O})_2$ to achieve a total concentration of 1.5 mM in SSF, the mixture was stored in an incubator shaker (Grant GLS 400, Grant Instruments, England) at 37 °C shaking at 50 rpm for 2 min to mimic the agitation in the oral cavity. Then, the oral "bolus" was added (1:1 v:v) to the preheated (37 °C) simulated gastric fluid (SGF, with $\text{CaCl}_2(\text{H}_2\text{O})_2$ to a total concentration of 0.15 mM in SGF). Then, the pH was adjusted to 3, using 1.0 and 0.1 M HCl. This mixture was incubated at 37 °C shaking at 50 rpm for 120 min in the incubator shaker (Grant GLS 400) to simulate stomach conditions. To mimic the small intestinal stage, the pre heated (37 °C) simulated intestinal fluid (SIF, with $\text{CaCl}_2(\text{H}_2\text{O})_2$ to a total concentration of 0.6 mM in SIF) containing bile salt (to achieve 10 μM final concentration of bile salt in the reaction vessel) was added to the gastric chime (1:1 v:v) in the temperature controlled (37 °C) titration vessel (70 mL, Metrohm 6.1418.150) of pH-STAT (OMNIS Titrator 2.1001.0XX0). Then, the pH was adjusted to 7 by adding 1.0 and 0.1 M NaOH solution to the reaction vessel. The pancreatic enzyme was added to obtain 2000 U mL^{-1} lipase activity and pH was kept at 7.0 by titrating the digesta with 0.3 M NaOH solution into the reaction vessel for 120 min. It is notable that the shear or mixing strength is not mentioned in the INFOGEST protocol. Therefore, to test the effect of the stirrer bar size and speed on the simulated digestibility of the samples, two different shear were applied: low shear (Omnis software value 6, corresponding to 650 ± 50 rpm) and high shear (Omnis software value 8, corresponding to 850 ± 50 rpm), applying the 10 mm \times 5 mm, and 15 mm \times 6 mm stirrer bar, respectively. The OMNIS automatic titrator was operated using OMNIS Software 2.10.0.

The percentage of released free fatty acids (FFAs) was calculated using the volume of consumed NaOH (Eq. (1)). In this equation, it was assumed that lipase will hydrolyze two FFAs per triglyceride molecule (Li & McClements, 2010):

$$\text{FFA}\% = \frac{(V \text{ NaOH} * M \text{ NaOH} * MW \text{ lipid})}{2 * W \text{ lipid}} * 100 \quad (1)$$

where, V NaOH is the volume (L) of NaOH solution consumed to neutralize the FFAs produced, M NaOH is the molarity (M) of the NaOH solution used, Mw lipid is the average molecular mass of the triglycerides ($876.16 \text{ g mol}^{-1}$) and W lipid is the total mass (g) of lipid present in the sample used for titration. The volume of titrated NaOH for samples without oil (blank) was subtracted from oil and oleogel samples.

2.4.2. Second trial: The impact of oil amount on the FFA% applying the INFOGEST protocol under high shear

In this trial, the impact the amount of oil had on the FFA% was investigated using the INFOGEST protocol with high shear. Therefore, 1000, 800, and 250 mg sunflower oil (remainder filled to 5 g with MilliQ water) were used, and the tests were done as discussed in Section 2.4.1, with 0.1 M NaOH to neutralize the digesta.

2.5. Differential scanning calorimetry (DSC)

Thermal properties of EC, waxes, their mixture, sunflower oil, and oleogels were analyzed using a DSC823^e differential scanning calorimeter (Mettler Toledo, Columbus, USA) mounted with a TSO801RO sample robot (Mettler Toledo). Samples were prepared by carefully weighing 6–9 mg in 40- μ L aluminum DSC pans. EC was subjected to three subsequent heating/cooling cycles: (i) from 25 °C to 200 °C, then cooled to 100 °C, (ii) heated to 200 °C, then cooled to 100 °C, and (iii) heated to 200 °C, and cooled to 25 °C. The neat waxes were heated from 25 °C to 100 °C and then cooled to 25 °C, except the BW that was heated from –15 °C to 100 °C and then cooled back to –15 °C. The mixture of EC and SFW (without oil) was subjected to two subsequent heating/cooling cycles: (i) from 25 °C to 200 °C and then cooled to 25 °C, (ii) heated to 100 °C and cooled to 25 °C. The mixture of EC and other neat waxes (without oil) were heated from 25 °C to 200 °C and then cooled to 25 °C, except the mixture of EC and BW which heated from –15 °C to 200 °C and then cooled back to –15 °C. The oil sample or the oleogelator (s) in oil were heated from 0 °C to 200 °C and then cooled back to 0 °C. Samples were kept at starting temperature and between steps for 5 min and heated or cooled at 5 °C/min under nitrogen flow (50 mL min⁻¹). The peak melting and crystallization temperature were taken as the minimum and maximum value of heat flow during transition, respectively. Total peak enthalpy (ΔH) was calculated by integrating melting curves. Data were processed using STARe DB V9.00 software (Mettler Toledo).

2.6. Fluorescence microscopy

The microstructures of the digesta in the reaction vessel (intestinal phase after 1, 10, 30, and 120 min) gathered from the experiments mentioned in Section 2.4 were examined using a fluorescence microscope (AxioScope A1, Zeiss, Germany) and lighting unit (Zeiss HXP 120C). The fluorescent dye Nile Red (dissolved in isopropanol (0.1%, w/v)) was used to stain the oil phase. 50 μ L of the dye solution was added to 500 μ L of the digesta and mixed manually for 10 s. One drop of the mixture was pressed within glass slide and a glass cover slip and was observed using an Axiocam 305 color camera (Zeiss, Germany) immediately after collection using 20X/0.45 Ph2 objective lens (Zeiss, Germany) at room temperature. All samples were prepared in duplicate and at least 8 images per sample were obtained. Images were acquired using ZEN 3.2 Software (Zeiss), and processed using ImageJ software (NIH, USA).

2.7. Analysis of free fatty acids by HPLC-ELSD

Lipids were extracted from the digesta after 2 h of intestinal phase based on the previous method (Zhao, Mikkonen, Kilpeläinen, & Lehtonen, 2020), with some modifications. Proteins and polysaccharides in aliquots of either 1 or 2 mL of digesta were precipitated with 2 mL of ethanol. Thereafter, the sample was acidified and lipids were extracted with 5 mL heptane:diethyl ether mixture (80:20 v/v). Two replicate extractions were performed for one digesta. Free fatty acids were determined from the extracts by normal-phase high performance liquid chromatography combined with evaporative light scattering detection (ELSD) according to Lampi et al. (2015). A LiChrosorb diol column (5 μ m, 3 \times 100 mm, VDS optilab Chromatographie Technik GmbH, Berlin, Germany) was connected to Waters Alliance 2695 HPLC system

equipped with a Waters 2420 ELSD (Waters®, Milford, MA, USA). Compounds were eluted with a gradient from 0.06% to 2% IPA in heptane + 0.1% acetic acid for 25 min at a flow rate of 0.5 mL min⁻¹. Drift tube temperature was set to 60 °C, nebulizer temperature to 42 °C and gain was 10. Nebulization was performed with filtered air at 20 psi. The samples were run as duplicates. Quantification was performed according to external standard method using oleic acid in a range of 200 to 4000 ng/injection.

2.8. Data analysis

Each experiment was performed at least twice with two measurements per sample, unless otherwise stated. All results were expressed as the average and standard deviation of the measurements. The graphs produced by OriginLab (OriginPro Software, V2021, USA) and graphical abstract is created with BioRender.com (2022).

3. Results and discussion

3.1. Microstructure of the oleogels

The microstructure, crystal morphology, and crystal aggregates in the oleogels made with waxes and the network microstructure of oleogel made with EC is shown in Fig. 1. The observed microstructures are in agreement with the literature (Blake, Co, & Marangoni, 2014; Blake & Marangoni, 2015a–c; Chopin-Doroteo et al., 2011; Dassanayake, Kodali, Ueno, & Sato, 2009; Doan et al., 2017a; Gómez-Estaca, Pintado, Jiménez-Colmenero, & Cofrades, 2019). However, comparing Fig. 1A–E (corresponding to oleogels made with 5 wt% wax) to Fig. 1G–K (corresponding to oleogels made with 5 wt% waxes and 5 wt% EC) shows that addition of EC in a concentration lower than its critical gelling concentration (the minimal concentration required for oil gelation, which is 7 wt% in case of EC) to wax oleogels does not alter the overall network and crystal morphology of the waxes. Interestingly, the addition of EC to waxes reduced the size of big SFW crystals (Fig. 1A and Fig. 1G). This may be attributed to the fact that more viscous oil (caused by addition of EC to the oil) slows down SFW crystal growth, resulting in formation of smaller crystals. This is not the case of other waxes, including RBW, CAW, CLW, and BW, as they already have small crystals, and increasing viscosity of oil does not impact their crystal morphology. These images may indicate the occurrence of crystal-biopolymer co-existence (from wax and EC, respectively).

3.2. The rate and extent of digestion of oleogels following the INFOGEST method

Here, the INFOGEST protocol (Brodkorb et al., 2019) was exactly followed to simulate the oral, gastric, and intestinal phases. However, as the shear was not mentioned in the INFOGEST protocol, the effect of low and high shear on the digestibility was investigated. The higher shear increases the rate and extent of oil and oleogel digestibility (Fig. 2). Higher shear breaks the oleogels to smaller particles compared to lower shear (Fig. S1). However, even the smaller particles are larger than a few millimeters (as determined visually). A higher surface area, which is caused by the smaller particles, would increase the rate and extent of oil digestion because lipid digestion occurs only when pancreatic lipase is anchored to the surfaces of the lipid droplets and be in contact with triacylglycerol and diacylglycerol molecules (Golding et al., 2011; Sabet et al., 2021). Although high shear increases the lipolysis (FFA% release) of all samples, it is drastically affecting wax oleogels (Fig. 2C and Fig. 2D). While at low shear the final FFA% release of SFW and RBW oleogels reach only 5.9% and 8.9%, respectively, these values climb up to 17% and 18% at high shear, resulting in 3- and 2-fold increase. In addition, low shear causes approximately 80 min delay in the start of the lipolysis of these wax oleogels (Fig. 2C and Fig. 2D, vertical black line). This is because the sticky structure of wax oleogels are not easily

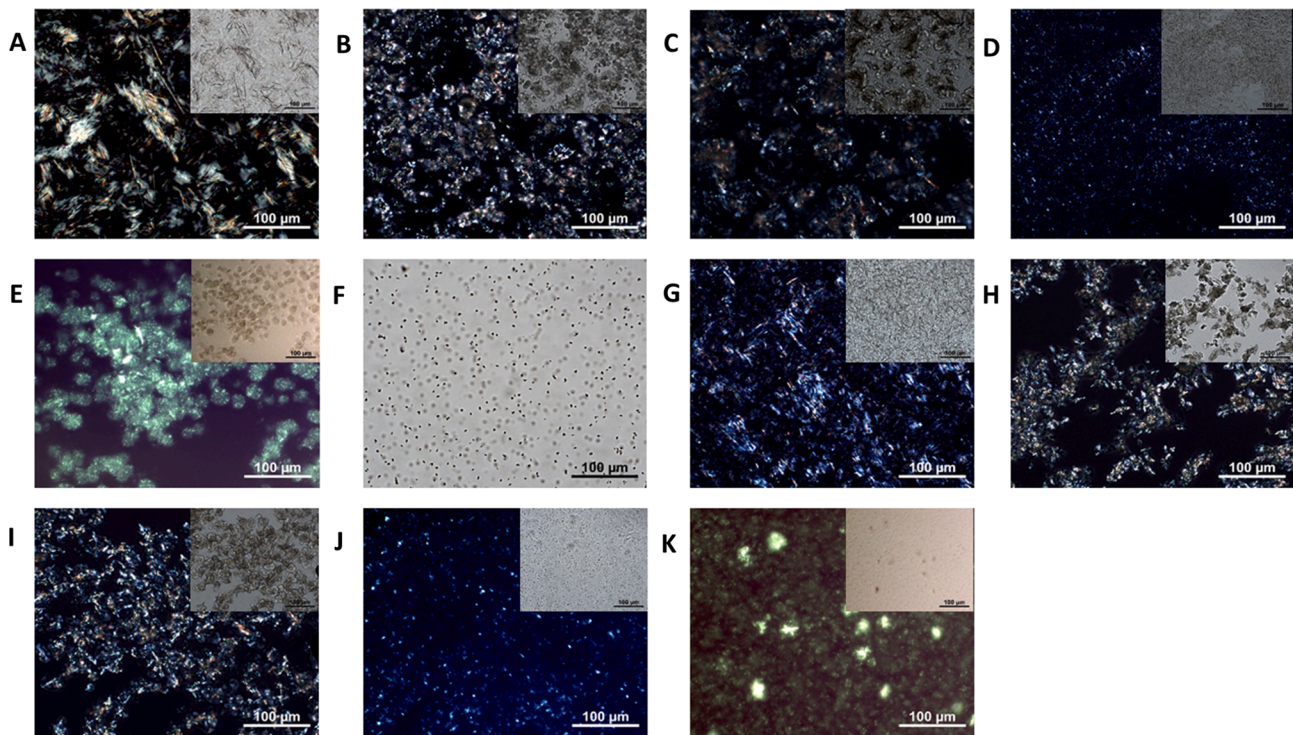


Fig. 1. Microstructure of wax oleogels (5 wt%, A to E), ethylcellulose (EC) oleogel (10 wt%, F), and wax plus EC oleogels (5 + 5 wt%, G to K) through polarized and bright-field images, main and inset, respectively. A: Sunflower wax oleogel, B: Rice bran wax oleogel, C: Carnauba wax oleogel, D: Candelilla wax oleogel, E: Berry wax oleogel, F: EC oleogel (only bright-field image is shown), G: Sunflower wax plus EC oleogel, H: Rice bran wax plus EC oleogel, I: Carnauba wax plus EC oleogel, J: Candelilla wax plus EC oleogel, K: Berry wax plus EC oleogel.

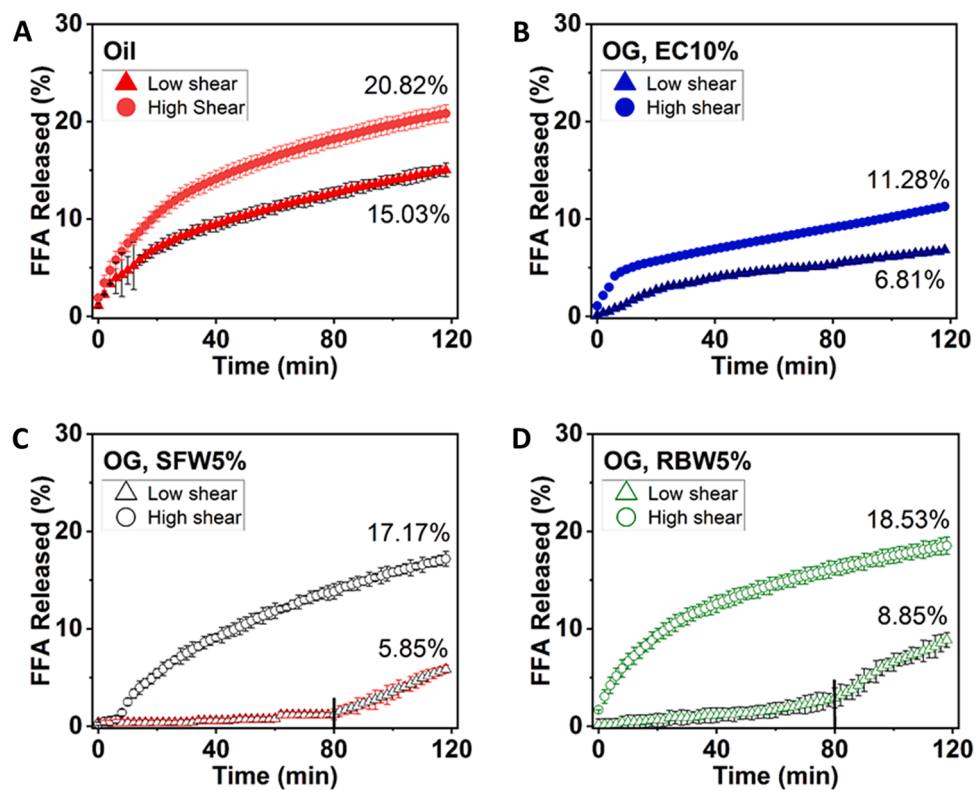


Fig. 2. The kinetics of free fatty acid (FFA) release from A: oil, B: 10 wt% ethylcellulose oleogel (EC), C: 5 wt% sunflower wax oleogel (SFW), and D: 5 wt% rice bran wax oleogel (RBW), while the INFOGEST protocol was followed at low and high shear in the titrator vessel. Percentages in figures indicate the final FFA value after digestion was completed. Vertical lines in panels C and D indicate a delay in lipolysis for low shear digestion.

disrupted by low shear. In contrast, the lipolysis of oil and EC oleogel is less affected by shear, where high shear causes 1.4- and 1.7-fold increase in FFA% compared to the low shear for oil and EC oleogel, respectively (Fig. 2A and Fig. 2B). This can be attributed to the fact that the oil can be disrupted to the small droplets with low shear and applying higher shear increases its disruption marginally. Moreover, the small particles of EC oleogel (10 wt%) have strong elastic (solid-like) structure, inhibiting them from disruption even at high shear.

It should be noted that in the explained experiments, the concentration of bile salt (10 μM) and pancreatic enzymes (2000 U mL^{-1} lipase activity) were too low compared to the lipid content of the samples (4.5 to 5 g). Therefore, expectedly, the lipolysis extent of oil and oleogels were less than 21% after 120 min of the exposure to the intestinal phase (Fig. 2). This may bring up the question about the reliability and comparability of these results. For example, we noticed that the FFA released of wax-EC oleogels, when 5 g oleogels are consumed and high shear is applied, reached 265–342% of that of oil (Fig. 3). This can be misleading as the solid structure of the wax-EC oleogel is supposed to hinder the lipolysis to some extent. Therefore, it is expected that the digestibility of oleogels to be lower than that of liquid oil. The lipolysis extent of oil, SFW, EC, and SFW-EC oleogels were also measured by HPLC-ELSD method at the end of the intestinal phase simulation. The trend of the FFA% achieved by HPLC-ELSD and titrator was similar in the case of oil, SFW and EC oleogels, but divergent in the case of SFW-EC oleogel (Fig. 3E). Expectedly and in contrast to the results of the titrator, the HPLC-ELSD results confirmed that the extent of lipolysis of SFW-EC oleogel is not higher than that of oil (Fig. 3E). The excessive NaOH consumption (and higher FFA release%) of SFW-EC oleogel compared to liquid oil can be due to (i) unknown acidic compounds (apart from the FFAs) in the SFW-EC oleogel and (ii) an artefact, which might happen due to the physical properties of gels, like a high volume of sticky gels.

3.3. The possible reasons for NaOH overconsumption for wax-EC oleogels during the intestinal phase simulation

As discussed in Section 2.2., wax oleogels were made by heating the components to 88 °C, whereas to make SFW-EC oleogels, gelators were heated to approximately 180 °C. Therefore, to check the effect of possible breakdown, oxidation, or any kind of heat-induced reactions on SFW at 180 °C, the SFW and oil (without EC) was heated at 180 \pm 5 °C for 15 min under stirring. Then it was cooled at room temperature overnight, following the same procedure for SFW-EC oleogel production. The lipolysis of the overheated SFW oleogel was like that of the SFW oleogel (data not shown). In addition, the DSC thermogram of neat SFW confirmed that there is no heat-induced reaction for this wax up to 185 °C (data not shown). Therefore, the high amount of NaOH consumption in the intestinal phase simulation of the SFW-EC oleogel did not originate from overheating SFW.

The chemical composition of waxes used in this study are different, e.g., SFW and RBW contain approximately 91–97 % wax ester (WE), 3–8% FFA, and less than 1% free fatty alcohol (FAL) and hydrocarbon (HC), in contrast to CLW that contains almost 73% HC, 16% WE, 9% FFA, and 2% FAL, and BW which contain almost 95% FFA, 4% FAL, and less than 1% WE and HC (Doan et al., 2017a). As the overconsumption of NaOH happened in the case of all waxes-EC oleogels, the chemical interaction between wax major components and EC at high temperature (which has not been studied yet) is very unlikely to be the reason for the overconsumption of NaOH. In addition, the polarized micrographs indicated the occurrence of wax crystal-biopolymer co-existence (Fig. 1). However, to exclude the probability of any heat-induced incidence between SFW and EC, the thermal events of neat EC, neat SFW, and their mixture in absence and in the presence of oil, in addition to their oleogels were studied using DSC (Fig. 4). The DSC thermogram obtained from EC showed a glass transition temperature (T_g), and vitrification process at around 130 °C, and 118 °C (in the first heating and cooling, respectively) (Fig. 4A), suggesting thermal hysteresis, which was in agreement with

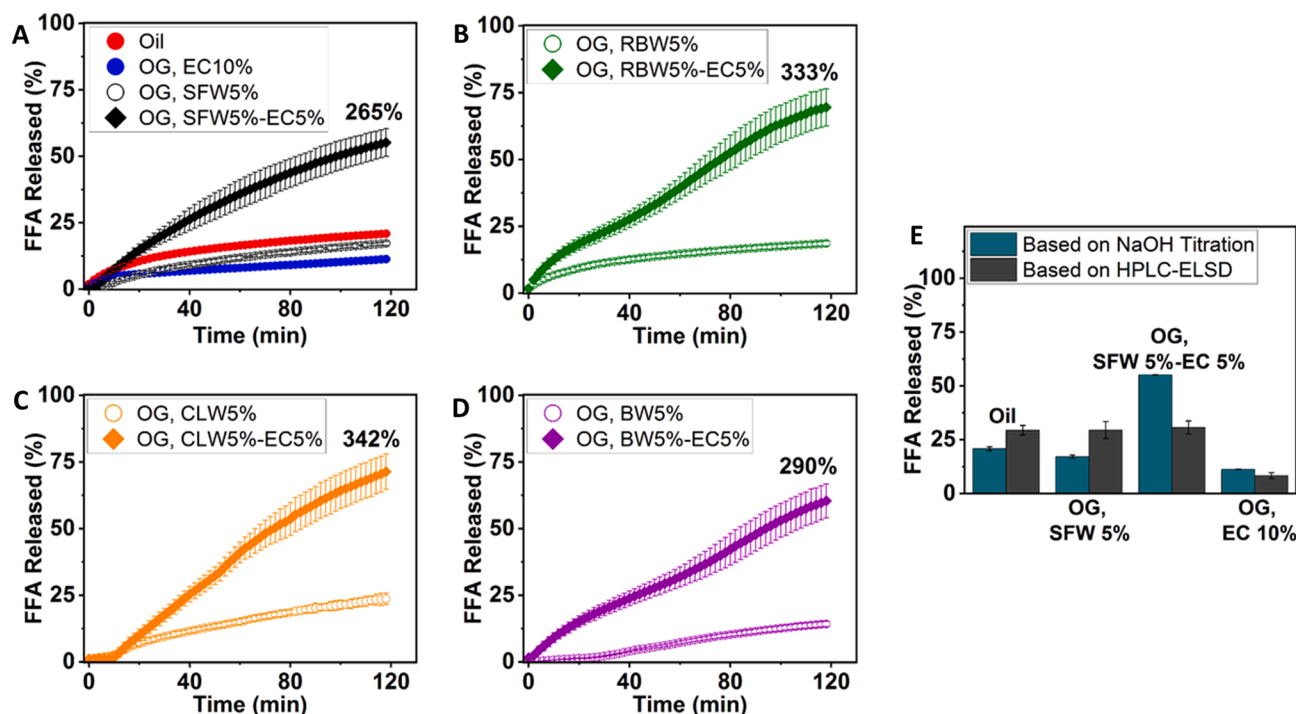


Fig. 3. The free fatty acid (FFA) release (%) over time (min) of the intestinal phase of oil and oleogels, when the INFOGEST protocol was followed. A: sunflower wax-ethylcellulose (SFW-EC) oleogel, B: Rice bran wax-ethylcellulose (RBW-EC) oleogel, C: Candelilla wax-ethylcellulose (CLW-EC) oleogel, D: Berry wax-ethylcellulose (BW-EC) oleogel, respectively, compared to those of oil, wax oleogel, and ethylcellulose oleogel. Percentages in figures indicate the percentage ratio between FFA value of wax-ethylcellulose oleogel in respect to the oil after digestion was completed. E: Comparison between FFA% obtained by NaOH consumption and HPLC-ELSD methods for oil, sunflower wax oleogel, sunflower wax-ethylcellulose oleogel, and ethylcellulose oleogel, when the INFOGEST protocol was followed.

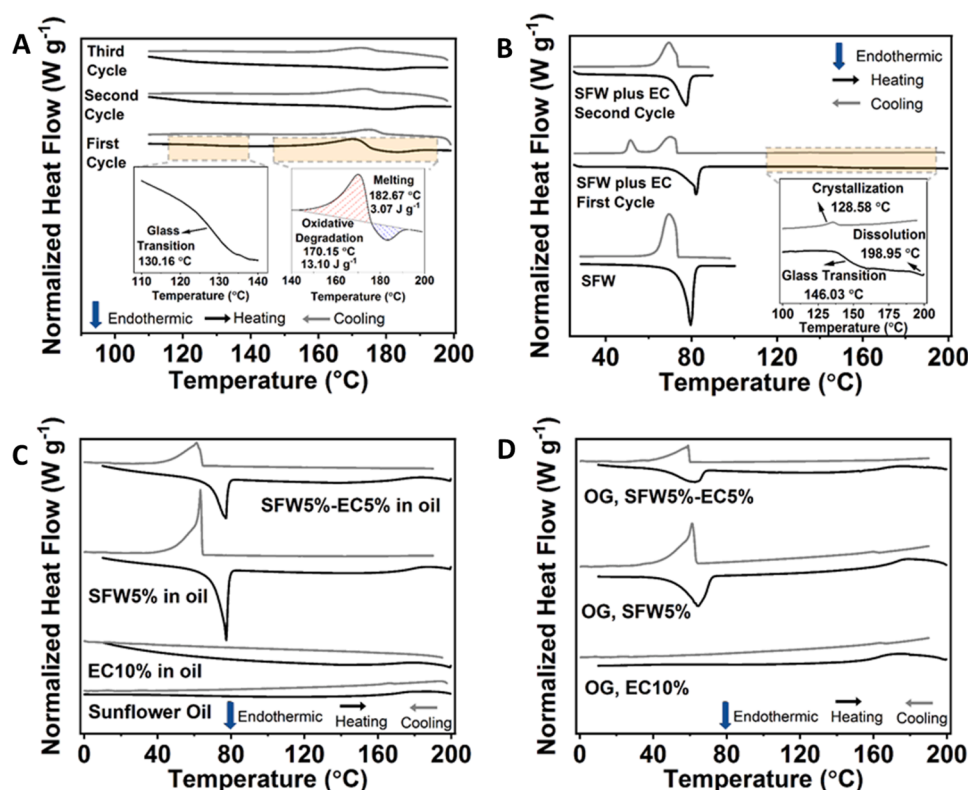


Fig. 4. A: DSC thermograms of ethylcellulose (EC) during first, second, and third heating and cooling cycles. Inset image at left shows the glass transition of EC in the first heating, and the inset at right shows oxidative degradation of EC followed by its dissolution. B: DSC thermograms of neat sunflower wax (SFW), and first and second cycles of neat SFW-EC. The inset image shows the glass transition, dissolution, and crystallization of EC portion in the mixture. C: DSC thermograms of sunflower oil, EC in the presence of sunflower oil, SFW in the presence of sunflower oil, and the mixture of SFW and EC in the presence of sunflower oil. D: DSC thermograms of oleogels made with EC, SFW, and their mixture. Endothermic, heating, and cooling are shown by blue, black, and grey arrows, respectively. (For interpretation of the references to color in this figure legend, the reader is referred to the web version of this article.)

literature (Davidovich-Pinhas, Barbut, & Marangoni, 2014). The T_g was not clearly observed in the second and third heating runs. It is known that local inhomogeneities causes a higher T_g (Roudaut, Simatos, Champion, Contreras-Lopez, & Le Meste, 2004). It is supposed that the T_g in the second and third heating runs are hidden in the lowering part of the baseline (Fig. 4A).

We also observed an exothermic thermal event at around 170 °C, which is followed by an endothermic thermal event at around 182 °C (Fig. 4A). Exothermic events in polymers are commonly attributed either to crystallization or with chemical alteration, such as degradation or cross linking (Lai, Pitt, & Craig, 2010). The exothermic behavior at 170 °C was not detected in the second and third cycles (Fig. 4A), confirming it is not a crystallization process. It is important to note that there is considerable variation in the behavior of EC at around 180 °C in the literature, which may be related to the difference in EC samples, their molecular weight, degree of substitution, preparation process, age, etc. Some authors did not observe the exothermic event at around 170–180 °C (Davidovich-Pinhas et al., 2014; Davidovich-Pinhas, Barbut, & Marangoni, 2015). In contrast, Dubernet, Rouland, & Benoit (1990), and Lai, Pitt, & Craig, (2010) mentioned the exothermic event at around 165 to 180 °C. This exothermic event corresponds to the oxidative degradation of EC (Lai et al., 2010). The following endothermic event (at around 182 °C) is associated with EC dissolution/melting which agrees with literature (Davidovich-Pinhas et al., 2014; Lai et al., 2010). In the first cooling, the crystallization phase transition, was detected at a lower temperature during cooling at around 174 °C, suggesting thermal hysteresis for this transition. The dissolution/melting and crystallization phase transitions and the hysteresis phenomenon occurred in the second heating and cooling runs, respectively, as well as the third cycle.

Neat SFW is mainly constituted of WE and FFAs (around 96% and 3%, respectively) (Doan et al., 2017a). Therefore, it has a narrow melting event at around 77 °C (Fig. 4B) in contrary to some other waxes, e.g., CLW which contains around 73%, 16%, 9%, and 2% of HC, WE, FFA, and FAL, respectively (Doan et al., 2017a), and has a wide melting event with a few distinct peaks (Fig. S2). There is no other heat-induced

event (such as oxidation or degradation) to be reported for neat SFW up to 200 °C, which means that SFW is a heat-stable wax. During cooling, crystallization was detected at around 71 °C (compared to 77 °C of melting phase transition), suggesting thermal hysteresis for this transition.

The combination of SFW (57.89 wt%) and EC (42.11 wt%), showed a higher melting point for SFW of around 81 °C, compared to that of the neat wax (77 °C). This behavior can be related to local inhomogeneity, caused by EC addition, which required WE and FFAs to require more thermal energy for melting. Moreover, the addition of SFW to EC increased the T_g of EC to 146 °C, compared to 130 °C for EC *per se*. It is supposed that the SFW present in the mixture would induce local inhomogeneities, which in return causes a higher T_g . The vitrification process was not clearly observed. Similarly, the oxidative degradation event of EC portion was not observed, which might be attributed to (i) the presence of major SFW compounds, i.e., WE and FFA inhibits the oxidation of EC to some extent (for example with oxygen scavenging effect), (ii) oxidative degradation of EC happens, but as the fraction of EC in the mixture is small (42.11 wt%) the oxidative degradation is not clearly observed. As the oxidative degradation of EC in a mixture with some other waxes, e.g., BW are more clearly observable but still less intense compared to pure EC (Fig. S2), we hypothesized that both phenomena might occur simultaneously. The melting event of EC portion in the SFW-EC mixture appears at around 198 °C, compared to that of 182 °C in the case of pure EC, which means SFW caused local inhomogeneities and increased the melting point. In addition, the crystallization phase transition of the EC portion, was detected at a lower temperature during cooling at around 128 °C, suggesting thermal hysteresis for this transition. The crystallization of the SFW in the mixture occurred showed an additional peak at 52 °C, compared to the single peak at 71 °C observed for neat SFW. Comparing the crystallization points of SFW portion in SFW-EC mixture (71 °C and 52 °C) to their melting point (81 °C), suggests a thermal hysteresis. In addition, the second cooling run of the SFW-EC mixture again showed two crystallization events at around 74 °C and 71 °C. These results may show that the

chemical interaction between EC (or EC oxidative products, such as peroxide, aldehydes, ketones, esters) with major SFW components, or the occurrence of the crystal-biopolymer co-existence (from wax and EC, respectively) can have an impact on the thermal event of neat SFW-EC mixture.

Thermal analysis of liquid sunflower oil did not reveal any characteristic thermal behavior apart from the oxidation (an exothermic event) at around 179 °C (Fig. 4C). Therefore, the exothermic events in Fig. 4C and Fig. 4D at around 179 °C can be assumed to be the effect of oil oxidation (with or without EC oxidation). The DSC thermograms of the EC and oil, SFW and oil, and EC plus SFW and oil were obtained by introducing the oil and powders directly into the DSC pan (Fig. 4C). Therefore, the heating and cooling runs in Fig. 4C correspond to dissolution and gelling stages of the oleogelators. In contrast, Fig. 4D shows the heating and cooling of oleogels previously made. The T_g of EC were not observed in the presence of oil (Fig. 4C) and in the previously made oleogel (Fig. 4D). In addition, the oxidation peak of EC either disappeared or it overlapped with the oxidation of oil. The fact that there is no thermal event during cooling of the mixture of EC and oil (Fig. 4C) and the heating of EC oleogel (Fig. 4D) is referred to the lack of highly ordered secondary structure (like the helix structures in gellan gum and agarose) (Davidovich-Pinhas et al., 2015). The DSC thermogram of SFW in the presence of oil showed a similar behavior to the neat SFW, with lower melting and crystallization temperatures (Fig. 4B and Fig. 4C). This is attributed to the dilution effect of oil, and in agreement with literature on other oleogels (Doan et al., 2017b; Valoppi, Calligaris, & Marangoni, 2016). In addition, the thermogram of SFW plus EC in the presence of oil is like that of SFW in the presence of oil (Fig. 4C). Similarly, the thermogram of SFW-EC oleogel is like that of SFW oleogel (Fig. 4D). This may be related to the lack of highly ordered secondary structure between SFW crystals and EC biopolymers.

Like SFW, the DSC thermograms of other neat waxes (RBW, CAW, CLW, and BW) revealed different behavior compared to when the EC is added to the neat waxes (Fig. S2). This may mean that EC biopolymer, to some extent, interferes with the crystallization of waxes. In contrast, the DSC thermogram of wax oleogels (SFW, RBW, CAW, CLW, and BW oleogels) were like those of wax-EC oleogels (SFW-EC, RBW-EC, CAW-EC, CLW-EC, and BW-EC oleogels) (Fig. 4C-D and Fig. S3). These may confirm the lack of a highly ordered secondary structure between SFW crystals and EC biopolymers, which agrees with the polarized micrographs (Fig. 1).

Overall, the DSC thermograms revealed no highly ordered secondary structure between wax crystals and EC biopolymers in the presence of oil. Therefore, although the probability of chemical interaction between EC or EC oxidative products with major wax components cannot be eliminated at this stage (and further studies are needed), these are very less likely to affect the NaOH overconsumption during the lipolysis of wax-EC oleogels. We hypothesized that the NaOH overconsumption happened by an artefact caused by the presence of a high amount of

sticky oleogels inside the vessel. If it is correct, lowering the amount of oil and oleogels in the titration vessel would resolve the problem. To test this hypothesis, we decreased the amount of oil and oleogels in the titrator vessel while the bile salt and pancreatic enzymes remained constant at the suggested amount by the INFOGEST protocol (Section 3.4).

3.4. Modifying INFOGEST protocol for digestibility studies of oleogel

As expected, lowering the amount of oil in the titration vessel, increased the lipolysis (Fig. 5A), which is attributed to the fact that a low amount of oil results in smaller oil droplets, higher surface area, and more severe interaction between bile salt/enzymes with oil droplets. It is notable that over 85% lipolysis is achieved when 250 mg oil was tested when the INFOGEST protocol was followed at high shear (Fig. 5A). Therefore, from now on all the oleogels used in this study contain 250 mg oil, so their lipolysis rate and extent can be compared with the crude oil.

Fig. 5B shows that even 5% EC in oil, (which appears as a viscous oil, not an oleogel) can reduce lipolysis to around 76%, compared to that of oil, which is approximately 86%. By increasing the concentration of EC to 10% (higher than its critical gelling concentration), the lipolysis extent is decreased to less than 55%. However, increasing EC concentration from 10% to 15%, did not reduce the lipolysis extent considerably. The elastic (solid-like) structure of oleogel with 10% and 15% EC can reduce the diffusion of enzymes and bile salt into the structure. Ashkar et al., (2019) also observed that the lipolysis of 8%, 10%, and 15% EC oleogels (all above its critical concentration) are not significantly different. However, they reported that the final lipolysis extent for EC oleogels (around 28%) is lower than ours (around 50%). This can be attributed to the different amount of oleogel, stirrer speed/size, and the enzyme concentrations used in these studies, which again confirms that there is the need for a standardized method for digestibility studies of oleogels.

The lipolysis rate and extent of the SFW and SFW-EC oleogels (each one contains 250 mg oil) were also investigated (Fig. 6A), using the same oleogels described in Section 3.2. As expected, the FFA% of SFW-EC oleogel (5%+5%) is between the upper and lower boundaries of SFW 5% and EC 10% oleogels. The FFA% of the samples at the end of the intestinal phase were also measured using HPLC-ELSD method (Fig. 6F). It is notable that the FFA% achieved from HPLC-ELSD and NaOH consumption methods are not supposed to be the same as they are different methods with different detection and calculation procedures. However, one may expect that the lipolysis extent achieved from these two methods should be in a similar trend for different oleogels. In contrary to Fig. 3E, the HPLC-ELSD results followed the same trend of NaOH consumption, when the amount of oil or oil content of oleogels is 250 mg (instead of 5 g). The results revealed that the lipolysis (and the NaOH consumption) of SFW-EC oleogel is not higher than that of oil, as

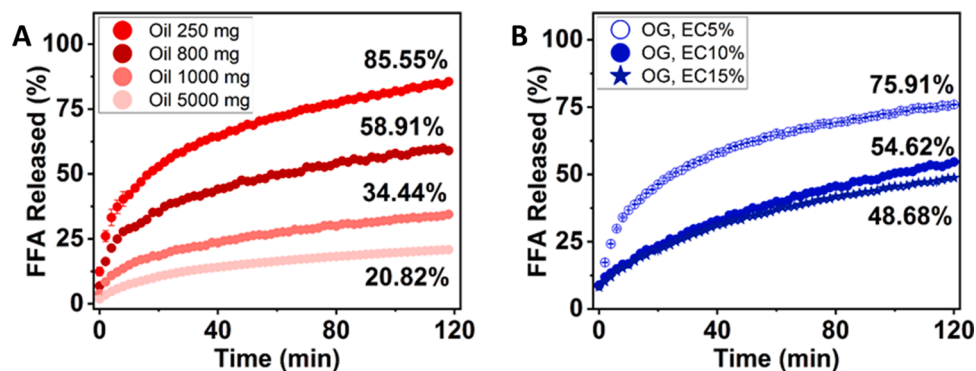


Fig. 5. A: The free fatty acid percentage (FFA%) released from different amounts of sunflower oil, when the INFOGEST protocol is applied. B: The FFA% released from ethylcellulose oleogels with 5, 10, and 15 wt%, compared to oil, when the modified version of INFOGEST is applied.

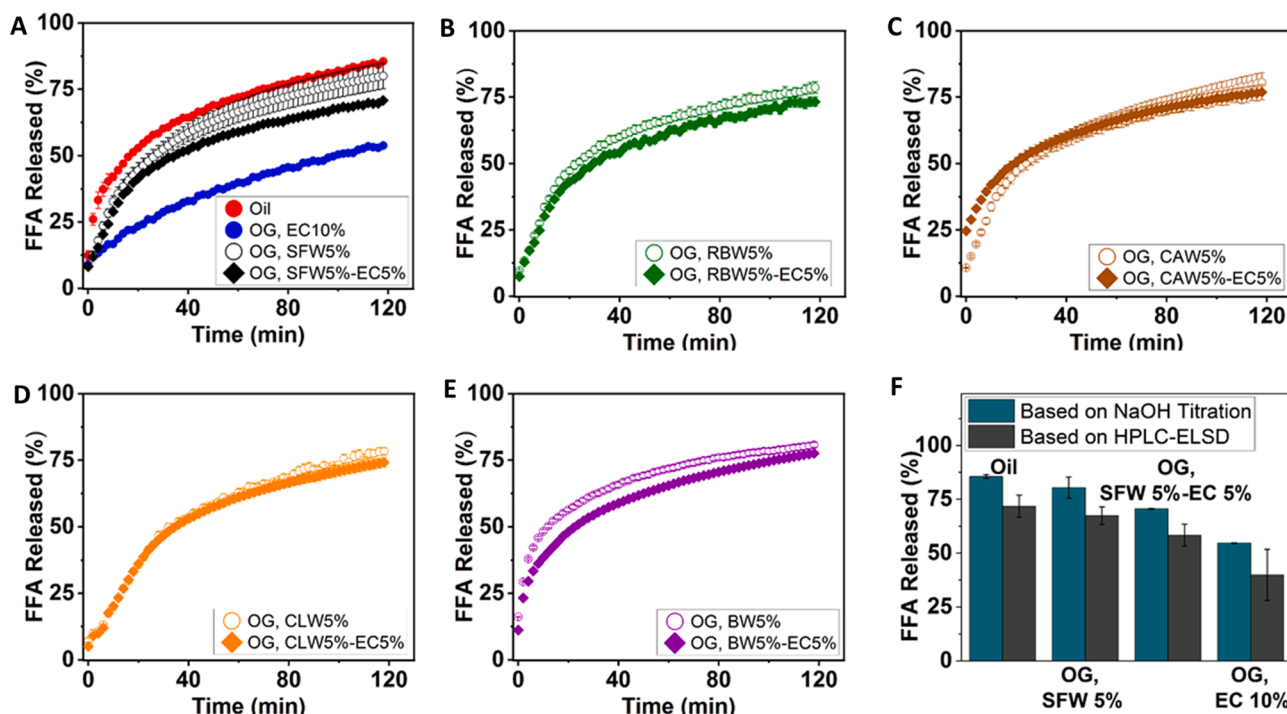


Fig. 6. The free fatty acid percentage (FFA%) released over time (min) of the intestinal phase of oil and oleogels, when the modified version of INFOGEST protocol was followed. A: sunflower wax-ethylcellulose (SFW-EC) oleogel, B: Rice bran wax-ethylcellulose (RBW-EC) oleogel, C: Carnauba wax-ethylcellulose (CAW-EC) oleogel, D: Candelilla wax-ethylcellulose (CLW-EC) oleogel, E: Berry wax-ethylcellulose (BW-EC) oleogel, respectively, compared to those of oil, wax, and ethylcellulose. F: The free fatty acid (FFA)% achieved by NaOH consumption and HPLC-ELSD methods for oil, sunflower wax oleogel, sunflower wax-ethylcellulose oleogel, and ethylcellulose oleogel, when the modified version of INFOGEST protocol was followed.

previously observed using the standard INFOGEST protocol (Fig. 3). This confirms that the origin of the overconsumption of NaOH was not a chemical interaction between present compounds. Indeed, if it was the case, it would also happen in the lower amount of oil and oleogels. Therefore, it might be a physical error attributed to the high amount of oleogels in the titration vessel. In addition, the results confirmed the oil content of the sample in the titration vessel affect the lipolysis rate and extent.

In addition, the lipolysis extent of other wax-EC oleogels is not higher than that of oil (Fig. 5B-E), which again confirmed the problem can be resolved by lowering the amount of oleogels in the titration vessel. In addition, the final digestibility of all wax oleogels is similar, around 75 to 80%, and no delay of digestion can be observed. This means that the chemical composition and crystal morphology of waxes do not affect the lipolysis of the entrapped oil.

As shown in Fig. 5, wax, EC, and wax-EC oleogels do not show a lag time (a time before the lipolysis starts). This means the elastic structure of these gels cannot restrict the penetration of bile salt and pancreatic enzymes into the structure. These results agree with previous study (Ashkar et al., 2019) in the case of EC oleogels, while contrast with Guo et al., (2019) in the case of RBW emulgel, where they reported 25 to 40 min delay before the starting of lipolysis. This can be due to applying different oil content, different stirrer bar speed and size, and different enzyme and bile salt concentration. Again, these variations between different studies further details the importance of a harmonized method for digestibility studies of oleogels.

At the beginning of the intestinal phase, all oleogels showed lumpy structure, where the oil content was entrapped inside (image not shown), which means their structure remained almost intact till the pancreatic enzymes are added. It means that the pH reversal from oral phase to gastric phase (7 to 3) and from gastric to intestinal phase (3 to 7) do not have a substantial influence on the oleogelators and the oleogel microstructure. As waxes and EC are hydrophobic in nature and do not

dissolve in water, the effect of pH on their surface charge (ζ -potential) is unknown. When the wax oleogels and EC oleogels enter the intestinal phase, they behave differently. For example, micrographs revealed that EC oleogel did not go through a harsh and quick lipolysis, and even after 120 min in the intestinal phase, it retained its overall structure (Fig. 7). The EC oleogel small particles were also visible by the naked eye at the end of the intestinal phase (image not shown). However, some big oil droplets were produced near the end of the intestinal phase experiment (Fig. 7). In addition, there was a short and quick rise in the lipolysis of EC oleogel at the beginning of the intestinal phase (Fig. 6) (reaches approximately 14.9 at 5 min in the intestinal phase). This indicates that there was some free oil on the surface of EC oleogel particles, which were possibly caused by shearing and rubbing on each other or the titrator vessel. However, after 5 min, the rate of FFA% release of EC oleogel remained almost constant (in contrary to wax oleogels and oil) (Fig. 6), which confirms that the microstructure of EC oleogel remains, to a certain extent, intact during the lipolysis, which is in agreement with the micrographs (Fig. 7). The enzymes and bile salt diffuse into the structure and the oil is lipolyzed. The products of the lipolysis, e.g., FFAs and monoglyceride also take some time to move outwards from the oleogel structure. Therefore, the lipolysis of EC oleogel (>7 wt% EC) follow the “interaction with enzymes and bile salts” pattern (Fig. 8).

In contrast to EC oleogels, a few seconds to minutes after the pancreatic enzymes were added to the titration vessel, the wax oleogels disintegrated into many small particles (image not shown). As shown in Fig. 7, the microstructure of wax oleogels faded over time in the intestinal phase, and oil droplets formed. Therefore, we hypothesize that the lipolysis of wax oleogels follow the “disintegration and interaction with enzymes and bile salts” pattern (Fig. 8). Moreover, there is no clear difference in the micrographs of oleogels made with different waxes (Fig. 7), and their rate and extent of lipolysis are similar (Fig. 6). These indicate that the chemical composition of wax, crystal morphology, and crystal distribution do not alter the digestibility of oil entrapped inside

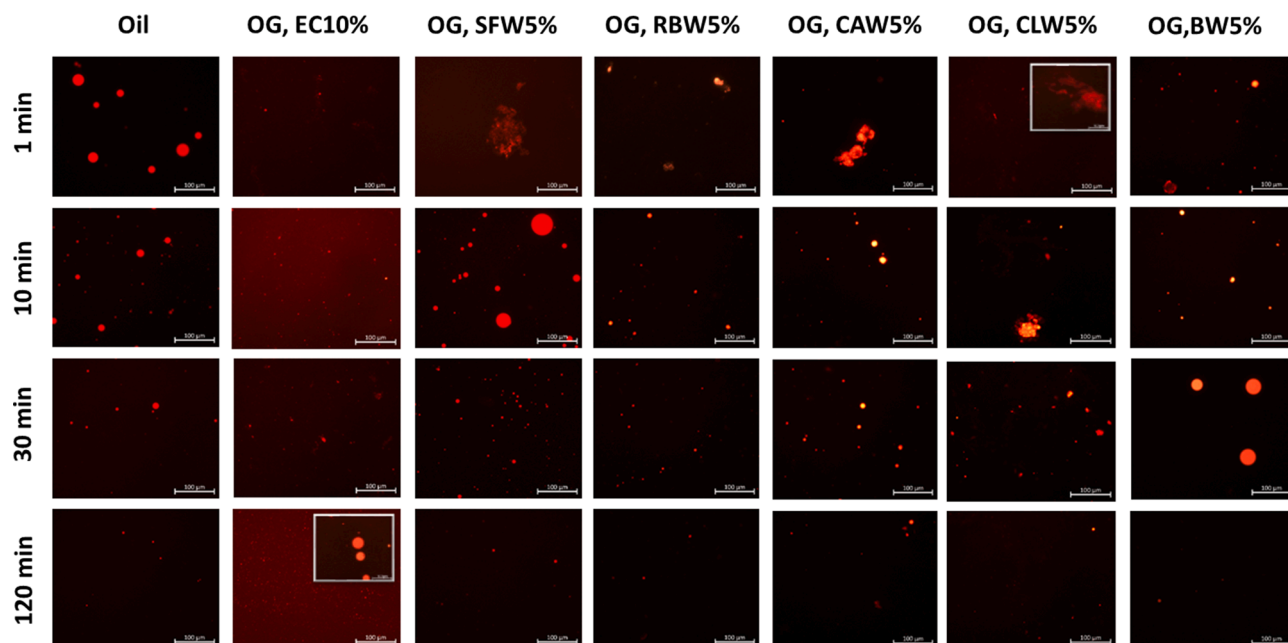


Fig. 7. The impact of simulated intestinal digestion on the microstructure of the oil and oleogels made with single oleogelator. The oil phases were stained red using Nile red. The scale bars represent 100 μm for all micrographs. OG EC, SFW, RBW, CAW, CLW, and BW represent ethylcellulose, sunflower wax, rice bran wax, carnauba wax, candelilla wax, and berry wax oleogels, respectively. As some of the samples are less homogeneous, the inset images show the less common aspects of the samples. (For interpretation of the references to color in this figure legend, the reader is referred to the web version of this article.)

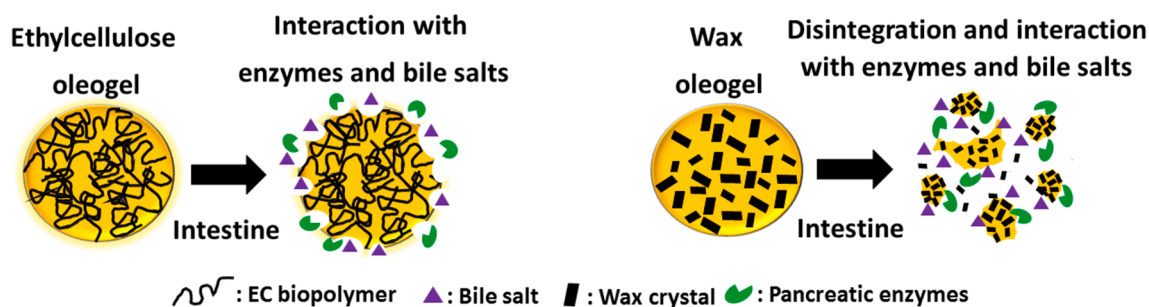


Fig. 8. A schematic presentation of the behavior of the ethylcellulose and wax oleogels under simulated intestinal tract conditions.

the wax crystals.

The micrographs of different wax-EC oleogels at one minute after the start of the intestinal phase are similar (Fig. 9), however, to a certain extent, different from those of wax oleogels (Fig. 7). Although the former commonly has a continuous bulky structure or bigger lumps (Fig. 9, 1 min), the latter (Fig. 7, 1 min) has smaller lumps with discontinuous structure. This difference apparently came from the effect of EC addition. However, after 30 min in the intestinal phase, the micrographs are like those of the wax oleogels.

3.5. A list of recommendations for a reliable application of INFOGEST static *in vitro* digestion protocol for oleogel analysis

To achieve more reliable results for static *in vitro* digestion of oleogels, some modifications need to be applied to the original INFOGEST protocol. Here we suggest a few minimal but fundamental changes along with some recommendations, which should be taken in consideration when using the INFOGEST protocol (Brodkorb et al., 2019) for oleogel digestion:

- The amount of oil in the oleogel chunk to be digested (or oil *per se*) should be 250 mg. Therefore, out of the 5 g sample (stated in the

INFOGEST protocol), add enough oleogel to reach 250 mg oil content (e.g., 277.8 mg oleogel with 10 % oleogelator) and the rest water.

- To avoid error (due to stickiness of oleogels to pH electrode or containers) perform the oral and gastric phases in the titrator vessel, not in beakers and shakers.
- Measure the volume of the oral bolus and gastric chyme in advance in a separate set of experiments. Therefore, you can add the required volume of SGF and SIF into the titration vessel.
- As the oleogels are commonly very sticky, the shear should be high enough to mix them thoroughly with the bile salt and enzymes. A round stirrer (without pivot ring) 15 mm \times 6 mm at speed 850 ± 50 rpm is recommended.
- The volume of titrated NaOH for samples without oil (blank) should be subtracted from the samples that consisted of oil and oleogels.
- The comparison between the results is only reliable when the FFA% release of oil (as reference) is at least 80% at the end of the intestinal phase.
- Use standardized NaOH solutions.

4. Conclusion

In this study, we showed that the standardized static *in vitro* INFOGEST protocol, which is designed to simulate the digestibility of

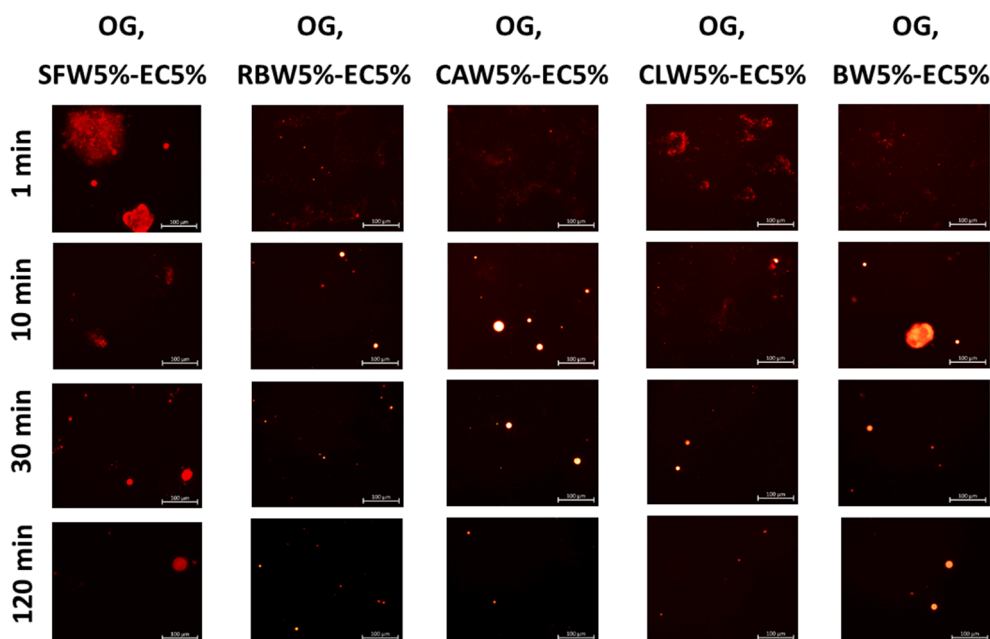


Fig. 9. The impact of simulated intestinal digestion on the microstructure of the oleogels made with a combination of wax and ethylcellulose. The oil phases were stained red using Nile red. The scale bars represent 100 μm for all micrographs. OG, EC, SFW, RBW, CAW, CLW, and BW represent oleogel, ethylcellulose, sunflower wax, rice bran wax, carnauba wax, candelilla wax, and berry wax, respectively. (For interpretation of the references to color in this figure legend, the reader is referred to the web version of this article.)

conventional foods, may not be applied for the lipolysis studies of oleogels with a high content (over 85 wt%) lipid. The oil content of oleogels and shear applied in the titration vessel alter the lipolysis rate and extent of oleogels. In addition, the NaOH consumption (during the intestinal digestion simulation) of wax-EC oleogels, when 5 g oleogels are consumed and high shear is applied, was significantly higher than that of oil, which is considered to be an artefact, that can be avoided by reducing the amount of oleogels in the titrator. We concluded the amount of oil (or oil in oleogels to be digested) should be 250 mg in order to achieve correct and reliable digestibility results using the INFOGEST protocol. We also highlighted that lipolysis of ethylcellulose oleogel follow the “interaction with enzymes and bile salts” pattern, whereas that of wax oleogel follow the “disintegration of oleogels and interaction with enzymes and bile salts”. We also noticed that the chemical composition of wax, crystal morphology, and crystal distribution do not alter the digestibility of oil entrapped inside the wax crystal network. In addition, we made some recommendations towards a more reliable application of INFOGEST static *in vitro* digestion protocol for oleogel analysis.

CRediT authorship contribution statement

Saman Sabet: Conceptualization, Methodology, Investigation, Formal analysis, Writing – original draft, Writing – review & editing, Visualization. **Satu J. Kirjoranta:** Investigation, Writing – review & editing. **Anna-Maija Lampi:** Investigation, Writing – review & editing. **Mari Lehtonen:** Investigation, Writing – review & editing. **Elli Pulkkinen:** Investigation, Writing – review & editing. **Fabio Valoppi:** Conceptualization, Resources, Methodology, Writing – review & editing, Project administration, Funding acquisition.

Declaration of Competing Interest

The authors declare that they have no known competing financial interests or personal relationships that could have appeared to influence the work reported in this paper.

Acknowledgements

The authors would also like to appreciate Mr Troy Faithfull for his valuable comments and English check.

Funding

The authors would like to acknowledge the Helsinki Institute for Life Science (FUN-OLEO project, decision letter number HY/2406/00.00.06.05/2019), and Jane and Aatos Erkkö Foundation (ENGEL project, grant number 200075) for their funding.

Appendix A. Supplementary material

Supplementary data to this article can be found online at <https://doi.org/10.1016/j.foodres.2022.111633>.

References

- Araiza-Calahorra, A., Glover, Z. J., Akhtar, M., & Sarkar, A. (2020). Conjugate microgel-stabilized Pickering emulsions: Role in delaying gastric digestion. *Food Hydrocolloids*, 105, Article 105794. <https://doi.org/10.1016/j.foodhyd.2020.105794>
- Ashkar, A., Laufer, S., Rosen-Kligvasser, J., Lesmes, U., & Davidovich-Pinhas, M. (2019). Impact of different oil gelators and oleogelation mechanisms on digestive lipolysis of canola oil oleogels. *Food Hydrocolloids*, 97, Article 105218. <https://doi.org/10.1016/j.foodhyd.2019.105218>
- Blake, A. I., Co, E. D., & Marangoni, A. G. (2014). Structure and physical properties of plant wax crystal networks and their relationship to oil binding capacity. *Journal of the American Oil Chemists' Society*, 91(6), 885–903. <https://doi.org/10.1007/s11746-014-2435-0>
- Blake, A. I., & Marangoni, A. G. (2015a). Plant wax crystals display platelet-like morphology. *Food Structure*, 3, 30–34. <https://doi.org/10.1016/j.foodstr.2015.01.001>
- Blake, A. I., & Marangoni, A. G. (2015b). The effect of shear on the microstructure and oil binding capacity of wax crystal networks. *Food Biophysics*, 10(4), 403–415. <https://doi.org/10.1007/s11483-015-9398-z>
- Blake, A. I., & Marangoni, A. G. (2015c). The use of cooling rate to engineer the microstructure and oil binding capacity of wax crystal networks. *Food Biophysics*, 10(4), 456–465. <https://doi.org/10.1007/s11483-015-9409-0>
- Brodkorb, A., Egger, L., Alminger, M., Alvito, P., Assuncao, R., Ballance, S., ... Recio, I. (2019). INFOGEST static *in vitro* simulation of gastrointestinal food digestion. *Nature protocols*, 14(4), 991–1014. <https://doi.org/10.1038/s41596-018-0119-1>
- Calligaris, S., Alongi, M., Lucci, P., & Anese, M. (2020). Effect of different oleogelators on lipolysis and curcuminoid bioaccessibility upon *in vitro* digestion of sunflower oil oleogels. *Food Chemistry*, 314, Article 126146. <https://doi.org/10.1016/j.foodchem.2019.126146>
- Carey, M. C., Small, D. M., & Bliss, C. M. (1983). Lipid digestion and absorption. *Annual review of physiology*, 45(1), 651–677. <https://doi.org/10.1146/annurev.ph.45.030183.003251>
- Chopin-Doroteo, M., Morales-Rueda, J. A., Dibildox-Alvarado, E., Charó-Alonso, M. A., de la Peña-Gil, A., & Toro-Vazquez, J. F. (2011). The effect of shearing in the thermo-mechanical properties of candelilla wax and candelilla wax–tripalmitin organogels. *Food Biophysics*, 6(3), 359–376. <https://doi.org/10.1007/s11483-011-9212-5>
- Davidovich-Pinhas, M., Barbut, S., & Marangoni, A. G. (2016). Development, characterization, and utilization of food-grade polymer oleogels. *Annual review of*

- food science and technology, 7, 65–91. <https://doi.org/10.1146/annurev-food-041715-033225>
- Davidovich-Pinhas, M., Barbut, S., & Marangoni, A. G. (2014). Physical structure and thermal behavior of ethylcellulose. *Cellulose*, 21(5), 3243–3255. <https://doi.org/10.1007/s10570-014-0377-1>
- Davidovich-Pinhas, M., Barbut, S., & Marangoni, A. G. (2015). The gelation of oil using ethyl cellulose. *Carbohydrate polymers*, 117, 869–878. <https://doi.org/10.1016/j.carbpol.2014.10.035>
- Dassanayake, L. S. K., Kodali, D. R., Ueno, S., & Sato, K. (2009). Physical properties of rice bran wax in bulk and organogels. *Journal of the American Oil Chemists' Society*, 86(12), 1163. <https://doi.org/10.1007/s11746-009-1464-6>
- Doan, C. D., Tavernier, I., Sintang, M. D. B., Danthine, S., Van de Walle, D., Rimaux, T., & Dewettinck, K. (2017b). Crystallization and gelation behavior of low-and high melting waxes in rice bran oil: A case-study on berry wax and sunflower wax. *Food Biophysics*, 12(1), 97–108. <https://doi.org/10.1007/s11483-016-9467-y>
- Doan, C. D., To, C. M., De Vrieze, M., Lynen, F., Danthine, S., Brown, A., ... Patel, A. R. (2017a). Chemical profiling of the major components in natural waxes to elucidate their role in liquid oil structuring. *Food Chemistry*, 214, 717–725. <https://doi.org/10.1016/j.foodchem.2016.07.123>
- Dubernet, C., Rouland, J. C., & Benoit, J. P. (1990). Comparative study of two ethylcellulose forms (raw material and microspheres) carried out through thermal analysis. *International journal of pharmaceuticals*, 64(2–3), 99–107. [https://doi.org/10.1016/0378-5173\(90\)90258-6](https://doi.org/10.1016/0378-5173(90)90258-6)
- Dupont, D., Bordonni, A., Brodtkorb, A., Capozzi, F., Cirkovic Velickovic, T., Corredig, M., ... Wickham, M. (2011). An international network for improving health properties of food by sharing our knowledge on the digestive process. *Food Digestion*, 2(1–3), 23–25. <https://doi.org/10.1007/s13228-011-0011-8>
- Egger, L., Ménard, O., Baumann, C., Duerr, D., Schlegel, P., Stoll, P., ... Portmann, R. (2019). Digestion of milk proteins: Comparing static and dynamic in vitro digestion systems with in vivo data. *Food Research International*, 118, 32–39. <https://doi.org/10.1016/j.foodres.2017.12.049>
- Egger, L., Ménard, O., Delgado-Andrade, C., Alvito, P., Assunção, R., Balance, S., ... Portmann, R. (2016). The harmonized INFOGEST in vitro digestion method: From knowledge to action. *Food Research International*, 88, 217–225. <https://doi.org/10.1016/j.foodres.2015.12.006>
- Gallego-Lobillo, P., Ferreira-Lazarte, A., Hernández-Hernández, O., & Villamiel, M. (2021). In vitro digestion of polysaccharides: InfoGest protocol and use of small intestinal extract from rat. *Food Research International*, 140, Article 110054. <https://doi.org/10.1016/j.foodres.2020.110054>
- Golding, M., Wooster, T. J., Day, L., Xu, M., Lundin, L., Keogh, J., & Clifton, P. (2011). Impact of gastric structuring on the lipolysis of emulsified lipids. *Soft matter*, 7(7), 3513–3523. <https://doi.org/10.1039/C0SM01227K>
- Gómez-Estaca, J., Pintado, T., Jiménez-Colmenero, F., & Cofrades, S. (2019). Assessment of a healthy oil combination structured in ethyl cellulose and beeswax oleogels as animal fat replacers in low-fat, PUFA-enriched pork burgers. *Food and Bioprocess Technology*, 12(6), 1068–1081. <https://doi.org/10.1007/s11947-019-02281-3>
- Guo, Q., Wijarnprecha, K., Sonwai, S., & Rousseau, D. (2019). Oleogelation of emulsified oil delays in vitro intestinal lipid digestion. *Food Research International*, 119, 805–812. <https://doi.org/10.1016/j.foodres.2018.10.063>
- Hur, S. J., Lim, B. O., Decker, E. A., & McClements, D. J. (2011). In vitro human digestion models for food applications. *Food chemistry*, 125(1), 1–12. <https://doi.org/10.1016/j.foodchem.2010.08.036>
- Infantes-García, M. R., Verkempinck, S. H. E., Gonzalez-Fuentes, P. G., Hendrickx, M. E., & Grauwet, T. (2021). Lipolysis products formation during in vitro gastric digestion is affected by the emulsion interfacial composition. *Food Hydrocolloids*, 110, Article 106163. <https://doi.org/10.1016/j.foodhyd.2020.106163>
- Lai, H. L., Pitt, K., & Craig, D. Q. (2010). Characterisation of the thermal properties of ethylcellulose using differential scanning and quasi-isothermal calorimetric approaches. *International journal of pharmaceuticals*, 386(1–2), 178–184. <https://doi.org/10.1016/j.ijpharm.2009.11.013>
- Lampi, A. M., Damerat, A., Li, J., Moiso, T., Partanen, R., Forssell, P., & Piironen, V. (2015). Changes in lipids and volatile compounds of oat flours and extrudates during processing and storage. *Journal of Cereal Science*, 62, 102–109. <https://doi.org/10.1016/j.jcs.2014.12.011>
- Li, Y., & McClements, D. J. (2010). New mathematical model for interpreting pH-stat digestion profiles: Impact of lipid droplet characteristics on in vitro digestibility. *Journal of Agricultural and Food Chemistry*, 58(13), 8085–8092. <https://doi.org/10.1021/jf101325m>
- Marangoni, A. G., van Duynhoven, J. P. M., Acevedo, N. C., Nicholson, R. A., & Patel, A. R. (2020). Advances in our understanding of the structure and functionality of edible fats and fat mimetics. *Soft Matter*, 16, 289–306. <https://doi.org/10.1039/c9sm01704f>
- Mat, D. J., Le Feunteun, S., Michon, C., & Souchon, I. (2016). In vitro digestion of foods using pH-stat and the INFOGEST protocol: Impact of matrix structure on digestion kinetics of macronutrients, proteins and lipids. *Food Research International*, 88, 226–233. <https://doi.org/10.1016/j.foodres.2015.12.002>
- Minekus, M., Alminger, M., Alvito, P., Ballance, S., Bohn, T., Bourlieu, C., ... Brodtkorb, A. (2014). A standardised static in vitro digestion method suitable for food—an international consensus. *Food & function*, 5(6), 1113–1124. <https://doi.org/10.1039/C3FO60702J>
- O'Sullivan, C.M. (2016b). In-vitro bioaccessibility and stability of beta-carotene in ethylcellulose oleogels. Master's thesis. Canada: University of Guelph. <http://hdl.handle.net/10214/9716>
- O'Sullivan, C. M., Barbut, S., & Marangoni, A. G. (2016a). Edible oleogels for the oral delivery of lipid soluble molecules: Composition and structural design considerations. *Trends in Food Science & Technology*, 57, 59–73. <https://doi.org/10.1016/j.tifs.2016.08.018>
- Roudaut, G., Simatos, D., Champion, D., Contreras-Lopez, E., & Le Meste, M. J. I. F. S. (2004). Molecular mobility around the glass transition temperature: A mini review. *Innovative Food Science & Emerging Technologies*, 5(2), 127–134. <https://doi.org/10.1016/j.ifset.2003.12.003>
- Sabet, S., Rashidinejad, A., Qazi, H. J., & McGillivray, D. J. (2021). An efficient small intestine-targeted curcumin delivery system based on the positive-negative-negative colloidal interactions. *Food Hydrocolloids*, 111, Article 106375. <https://doi.org/10.1016/j.foodhyd.2020.106375>
- Sanchón, J., Fernández-Tomé, S., Miralles, B., Hernández-Ledesma, B., Tomé, D., Gaudichon, C., & Recio, I. (2018). Protein degradation and peptide release from milk proteins in human jejunum. Comparison with in vitro gastrointestinal simulation. *Food chemistry*, 239, 486–494. <https://doi.org/10.1016/j.foodchem.2017.06.134>
- Santos-Hernández, M., Alfieri, F., Gallo, V., Miralles, B., Masi, P., Romano, A., ... Recio, I. (2020). Compared digestibility of plant protein isolates by using the INFOGEST digestion protocol. *Food Research International*, 137, Article 109708. <https://doi.org/10.1016/j.foodres.2020.109708>
- Sousa, R., Portmann, R., Dubois, S., Recio, I., & Egger, L. (2020). Protein digestion of different protein sources using the INFOGEST static digestion model. *Food Research International*, 130, Article 108996. <https://doi.org/10.1016/j.foodres.2020.108996>
- Tan, Y., Zhang, Z., Mundo, J. M., & McClements, D. J. (2020). Factors impacting lipid digestion and nutraceutical bioaccessibility assessed by standardized gastrointestinal model (INFOGEST): Emulsifier type. *Food Research International*, 137, Article 109739. <https://doi.org/10.1016/j.foodres.2020.109739>
- Torcello-Gómez, A., Dupont, D., Jardin, J., Briard-Bion, V., Deglaire, A., Risse, K., ... Mackie, A. (2020). Human gastrointestinal conditions affect in vitro digestibility of peanut and bread proteins. *Food & Function*, 11(8), 6921–6932. <https://doi.org/10.1039/D0FO01451F>
- Valoppi, F., Calligaris, S., & Marangoni, A. G. (2016). Phase transition and polymorphic behavior of binary systems containing fatty alcohols and peanut oil. *Crystal Growth & Design*, 16(8), 4209–4215. <https://doi.org/10.1021/acs.cgd.6b00145>
- Verkempinck, S. H. E., Salvia-Trujillo, L., Moens, L. G., Charleer, L., Van Loey, A. M., Hendrickx, M. E., & Grauwet, T. (2018). Emulsion stability during gastrointestinal conditions effects lipid digestion kinetics. *Food chemistry*, 246, 179–191. <https://doi.org/10.1016/j.foodchem.2017.11.001>
- Versantvoort, C. H., Oomen, A. G., Van de Kamp, E., Rempelberg, C. J., & Sips, A. J. (2005). Applicability of an in vitro digestion model in assessing the bioaccessibility of mycotoxins from food. *Food and chemical toxicology*, 43(1), 31–40. <https://doi.org/10.1016/j.fct.2004.08.007>
- Wang, S., Chen, K., & Liu, G. (2021). Monoglyceride oleogels for lipophilic bioactive delivery—influence of self-assembled structures on stability and in vitro bioaccessibility of astaxanthin. *Food Chemistry*, 131880. <https://doi.org/10.1016/j.foodchem.2021.131880>
- Zhao, H., Mikkonen, K. S., Kilpeläinen, P. O., & Lehtonen, M. I. (2020). Spruce Galactoglucomannan-Stabilized Emulsions Enhance Bioaccessibility of Bioactive Compounds. *Foods*, 9(5), 672. <https://doi.org/10.3390/foods9050672>
- Zhou, H., Dai, T., Liu, J., Tan, Y., Bai, L., Rojas, O. J., & McClements, D. J. (2021). Chitin nanocrystals reduce lipid digestion and β-carotene bioaccessibility: An in-vitro INFOGEST gastrointestinal study. *Food Hydrocolloids*, 113, Article 106494. <https://doi.org/10.1016/j.foodhyd.2020.106494>
- Zhou, H., Hu, Y., Tan, Y., Zhang, Z., & McClements, D. J. (2021). Digestibility and Gastrointestinal Fate of Meat versus Plant-Based Meat Analogs: An In Vitro Comparison. *Food Chemistry*, 130439. <https://doi.org/10.1016/j.foodchem.2021.130439>